

## Low-temperature structural change and magnetic anomaly in superconducting $\text{Cd}_2\text{Re}_2\text{O}_7$

Hironori Sakai,\* Harukazu Kato, Shinsaku Kambe, and Russell E. Walstedt  
*Advanced Science Research Center, Japan Atomic Energy Research Institute, Tokai, Ibaraki 319-1195, Japan*

Hiroyuki Ohno, Masaki Kato, and Kazuyoshi Yoshimura  
*Department of Chemistry, Graduate School of Science, Kyoto University, Kyoto 606-8502, Japan*

Hirofumi Matsuhata  
*Division of Electronics, National Institute of Advanced Industrial Science and Technology, Tsukuba, Ibaraki 305-8568, Japan*  
 (Received 15 April 2002; published 30 September 2002)

The structural phase transition at  $T^* \sim 200$  K in the superconducting pyrochlore oxide  $\text{Cd}_2\text{Re}_2\text{O}_7$  has been investigated using x-ray and electron diffraction experiments and  $^{111}\text{Cd}$ -NMR (nuclear-magnetic-resonance) measurements. The susceptibility for  $\text{Cd}_2\text{Re}_2\text{O}_7$  in the high-temperature region ( $T \gg T^*$ ) obeys a Curie-Weiss law with a large and negative Weiss temperature, which indicates that this system possesses a localized-moment nature with antiferromagnetic interactions, leading to geometrical frustration. X-ray and electron-diffraction measurements suggest the tetramerization of Re below  $T^*$ , which induces a nanosized stripe structure. From  $^{111}\text{Cd}$ -NMR experiments, a large orbital susceptibility is identified by means of a  $K\chi$  plot. Both the spin susceptibility and  $(T_1T)^{-1}$  are found to decrease sharply below  $T^*$ , signaling a decrease in density of states, which is apparently caused by a developing partial energy gap at the Fermi surface.

DOI: 10.1103/PhysRevB.66.100509

PACS number(s): 74.70.-b, 74.25.Ha, 61.14.-x, 76.60.-k

Recently, the pyrochlore oxide  $\text{Cd}_2\text{Re}_2\text{O}_7$  has been found to exhibit type-II superconductivity at  $\sim 1.1$  K.<sup>1,2</sup> This discovery has triggered investigations of the relation between superconductivity and exchange bond frustration. The pyrochlore oxides  $A_2B_2O_7-\delta$  encompass a large number of compounds depending on the choice of elements A and B, as in the case of perovskite oxides. These compounds exhibit a wide variety of physical properties ranging from insulator through semiconductor and from bad metal to good metal.<sup>3</sup> However, before the recent  $\text{Cd}_2\text{Re}_2\text{O}_7$  work, no superconductivity had been reported for pyrochlore oxides.

Pyrochlore oxide structures include a three-dimensional (3D) tetrahedral network of the magnetic  $B$  cations, that is, the so-called *pyrochlore lattice*. If the  $A$  cations are nonmagnetic and the  $B$  cations are antiferromagnetically coupled, the  $B$ -spin magnetic couplings are strongly frustrated under a nearest-neighbor exchange interaction on this lattice. In recent years, there has been renewal of interest in these geometrically frustrated systems, since the metallic spinel oxide  $\text{LiV}_2\text{O}_4$ , which has a pyrochlore lattice of vanadium, was reported to exhibit heavy-fermion behavior at low temperatures due to the geometrical frustration.<sup>4</sup>

$\text{Cd}_2\text{Re}_2\text{O}_7$  undergoes a second-order structural phase transition at  $T^* \sim 200$  K, i.e., from a high-temperature (HT) phase with the cubic pyrochlore structure (space group  $Fd\bar{3}m$ ) to a low-temperature (LT) phase with another cubic structure which is still unidentified.<sup>5</sup> Below  $T^*$ , the resistivity and susceptibility both decrease steeply with decreasing temperature. The nature of the LT phase is important, since the frustration can be released in some manner in the LT phase, and this release is a possible cause for the structural change. Some properties of the LT phase have already been studied. Band calculations for the cubic pyrochlore structure predict that this compound is a compensated semimetal with

very low carrier density, and that the Fermi level  $E_F$  lies in the Re  $5d$  band, giving an electronic specific heat coefficient  $\gamma \sim 2.7$  mJ K<sup>-2</sup>/Re mol.<sup>6</sup> However, the experimental  $\gamma$  ( $T \rightarrow 0$ ) has been reported to be 13–15 mJ K<sup>-2</sup>/Re mol,<sup>2,7,8</sup> indicating that substantial renormalization of the effective mass occurs in this system. Indeed, in the normal state, the  $T^2$  dependence of resistivity ( $\rho = \rho_0 + AT^2$ ) in the low-temperature region suggests that this system behaves as a correlated Fermi liquid.<sup>9</sup> Furthermore, in the superconducting state the large initial slope of the upper critical field  $H_{c2}$  suggests that the Cooper pairs are composed of rather heavy quasiparticles.<sup>1</sup>

In order to clarify the nature of the structural transition and the electronic change of state through  $T^*$ , we have performed  $^{111}\text{Cd}$ -NMR (nuclear-magnetic-resonance) measurements. We have also investigated the magnetic susceptibility and the x-ray and electron-diffraction patterns above and below  $T^*$ , utilizing single-crystal samples. Powder samples and single crystals of  $\text{Cd}_2\text{Re}_2\text{O}_7$  were prepared by solid-state reaction<sup>1</sup> and by chemical transport reaction with iodine as a transporter, respectively.

Let us start with the magnetism in the HT phase. The susceptibility of the single crystalline  $\text{Cd}_2\text{Re}_2\text{O}_7$  was measured using a superconducting quantum interference device magnetometer in the temperature range 2–300 K, and a torsion-balance magnetometer above room temperature (RT). Figure 1 shows the temperature dependence of the magnetic susceptibility  $\chi$  and its inverse  $\chi^{-1}$  for  $\text{Cd}_2\text{Re}_2\text{O}_7$  together with those of the related pyrochlore ruthenates. The  $\chi^{-1}$  of  $\text{Cd}_2\text{Re}_2\text{O}_7$  above  $\sim 400$  K is linearly dependent on temperature; that is, it obeys a Curie-Weiss (CW) law with a large, negative Weiss temperature  $\Theta \sim -1500$  K. The Curie constant leads to an effective magnetic moment of  $1.88\mu_B/\text{Re}$ , which is close to the estimated free ion value ( $1.73\mu_B$ ) for

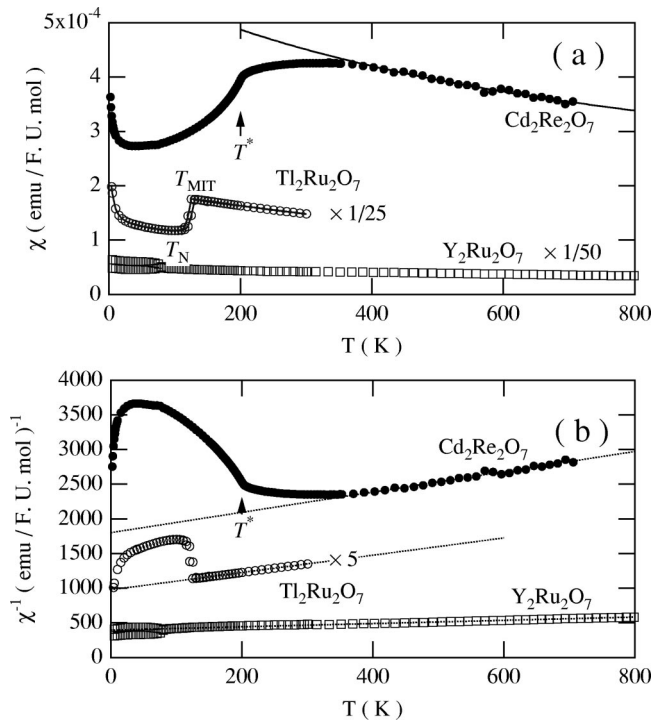


FIG. 1. Temperature dependence of (a) magnetic susceptibility and (b) inverse susceptibility for  $\text{Cd}_2\text{Re}_2\text{O}_7$ ,  $\text{Y}_2\text{Ru}_2\text{O}_7$ , and  $\text{Tl}_2\text{Ru}_2\text{O}_7$ .

$S=1/2$ , although spin  $S=1$  is expected for the  $5d^2$  state of Re in this compound. The negative Weiss temperature indicates that the local exchange interactions are antiferromagnetic.

For comparison, the data for the pyrochlore ruthenates  $\text{Y}_2\text{Ru}_2\text{O}_7$  and  $\text{Tl}_2\text{Ru}_2\text{O}_7$  are included in Fig. 1.  $\text{Y}_2\text{Ru}_2\text{O}_7$  is known to be a Mott insulator having localized magnetic moments on the  $\text{Ru}^{4+}$  cations ( $S=1$ ) with a large, negative  $\Theta \sim -1100$  K.<sup>10</sup> This system exhibits long-range order with a complicated magnetic structure ( $T_N=76.5$  K) due to the spin frustration.<sup>11</sup> In  $\text{Tl}_2\text{Ru}_2\text{O}_7$ , an abrupt metal-insulator transition (MIT) takes place at  $T_{\text{MIT}}=120$  K.<sup>12</sup> Even in the metallic phase, the susceptibility of  $\text{Tl}_2\text{Ru}_2\text{O}_7$  obeys a CW law, where the  $\Theta$  is also large and negative:  $\Theta \sim -600$  K. We note that the ground state of this insulating phase has been suggested to be a spin singlet.<sup>13</sup> The large, negative  $\Theta$  can be regarded as a characteristic feature of pyrochlore oxides with antiferromagnetic interactions since the  $\Theta$ , which represents the energy scale of the nearest-neighbor exchange interactions in a molecular-field approximation, has been noted to be typically large on the frustrated pyrochlore lattice.<sup>14</sup>

Meanwhile, CW behavior in metallic compounds can be explained in terms of the average amplitude of the local spin fluctuations  $\langle S_L^2 \rangle$ , which when Fourier transformed becomes the  $q$ -dependent susceptibility  $\chi_q$ , where  $q$  is the wave vector. CW behavior is seen in the following cases: (i) nearly or weakly ferromagnetic metals such as  $\text{ZrZn}_2$  (Ref. 15) where  $\chi_q$  is enhanced only for small  $q$  and  $\langle S_L^2 \rangle$  is proportional to temperature; (ii) robust localized-moment systems such as the Mn Heusler alloy  $\text{In}_2\text{MnGa}$ ,<sup>16</sup> where  $\chi_q$  is almost  $q$ -independent and  $\langle S_L^2 \rangle \sim S(S+1)$ ; and (iii) temperature induced

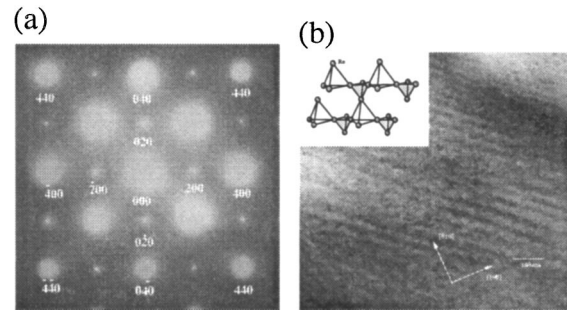


FIG. 2. (a) Electron-diffraction pattern for  $\text{Cd}_2\text{Re}_2\text{O}_7$  at  $T=120$  K. (b) TEM images at  $T=120$  K corresponding to (a). The inset of (b) shows the possible Re network of the LT phase.

local moment systems such as  $\text{CoSe}_2$ ,<sup>17</sup> where  $\langle S_L^2 \rangle$  increases with increasing temperature and approaches a constant value at high-temperatures. The CW behavior of  $\text{Cd}_2\text{Re}_2\text{O}_7$  can be categorized as either case (ii) or (iii), because the observed effective moment is not so small, and the resistivity becomes large and almost temperature independent above  $T^*$ . In any case,  $\text{Cd}_2\text{Re}_2\text{O}_7$  appears to possess a localized-moment character; thus, geometrical frustration effects should persist in the high temperature region above  $T^*$ . From the viewpoint of band structure, Re  $5d$  electrons are dominant in the density of states at  $E_F$ , which is located near the valley of the  $5d$  band.<sup>6</sup> The  $5d$  band shows sharp peaks in the density of states just below  $E_F$ . This peaked and narrow band result supports the existence of localized-moment character for the Re  $5d$  electrons.

Next, turning to the structural change at  $T^*$ , superlattice reflections are clearly observed below  $T^*$  in powder x-ray-diffraction (XRD) patterns and also in electron-diffraction patterns observed using a transmission-type electron microscope (TEM). Figure 2(a) shows the electron-diffraction patterns for  $\text{Cd}_2\text{Re}_2\text{O}_7$  along the  $[001]$  zone axis at 120 K. The corresponding TEM images are also indicated in Fig. 2(b). The XRD and electron-diffraction patterns at RT are consistent with the cubic pyrochlore structure ( $Fd\bar{3}m$ ). At 120 K, well below  $T^*$ , superlattice reflections are clearly observed, e.g., at  $(200)$  and  $(240)$  positions as Jin *et al.* already have reported.<sup>18</sup> These superlattice reflections indicate a doubling of the periodic crystal structure along each crystal axis in comparison with the cubic pyrochlore structure. To determine the precise crystal structure of the LT phase, we have measured convergent-beam electron-diffraction patterns. Since a convergent beam irradiates an extremely small domain, this technique offers data with which to decide the space group for a new material or unknown phase. However, not even the space group could be determined up to now because of the following particularity in the LT phase. Below  $T^*$  at 120 K, as seen in Fig. 2(b), dark and bright fringes emerge quite clearly with a spacing of about  $20$  Å for each mosaic domain, which may be due to some lattice defects. It is equally possible that these fringes could be caused by nanosize stripe microstructure, which would also cause difficulty in determining a detailed crystal structure, since the existence of the stripe microstructure even in a convergent area of an electron beam leads to a complicated diffraction

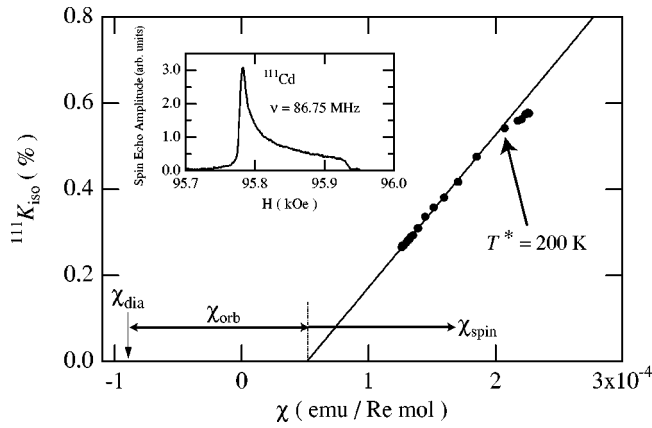


FIG. 3.  $^{111}\text{Cd}$  isotropic Knight shift plotted against the observed susceptibility with temperature as an implicit parameter. The inset shows the  $^{111}\text{Cd}$ -NMR spectrum for  $\text{Cd}_2\text{Re}_2\text{O}_7$  at 1.8 K.

pattern. Beyond this, we have continued the structural analyses using XRD, TEM, and neutron diffraction experiments. Further investigations will be reported in detail elsewhere.

On the other hand, our preliminary XRD study for a single crystal using a four-circle x-ray diffractometer suggests that a slight expansion and contraction of tetrahedra occurs alternately in the noncubic Re pyrochlore lattice, as illustrated schematically in the inset of Fig. 2(b). A similar structural model has been advocated by Hanawa *et al.* as well.<sup>5</sup> This structural model is consistent with the observed twofold periodic superlattice, which would be caused by an alternating Re-Re bond length. The direction of the domains in TEM images is along  $\langle 110 \rangle$ , which corresponds to the direction of the Re network. Therefore, these microdomains are considered to be caused by the formation of an alternating sequence of expansion and contraction in the Re 3D network with different phases (+ - + - and - + - +). This model may also indicate certain charge modulations and fluctuations, because the variation of Re-Re bond length implies a varying valence for the Re.

Let us turn now to the  $^{111}\text{Cd}$ -NMR results. NMR measurements for a powder sample were performed using a phase-coherent type of pulsed spectrometer. Nuclear spin-lattice relaxation rates  $T_1^{-1}$  were measured by an inversion-recovery method for spin-echo signals following an inversion  $\pi$  pulse. The inset to Fig. 3 shows the NMR spectrum for  $^{111}\text{Cd}$  nuclei with nuclear spin  $I=1/2$  in  $\text{Cd}_2\text{Re}_2\text{O}_7$  at 1.8 K. We obtained a similar spectrum for the other stable isotope,  $^{113}\text{Cd}$ , also with  $I=1/2$ . Since NMR spectra for  $I=1/2$  are free of nuclear electric quadrupole effects, the observed asymmetric spectrum is a typical powder pattern due to an anisotropic Knight shift  $K_{\text{aniso}}$ . Therefore, the sharp peak and the small step on the right side of the spectrum correspond to  $K_{\perp}$  and  $K_{\parallel}$ , perpendicular to and along the symmetry axis of Cd site, respectively. The spectral width ( $\sim |K_{\parallel} - K_{\perp}| = \frac{3}{2} |K_{\text{aniso}}|$ ) is almost independent of temperature, and is about 0.16%, leading to  $|K_{\text{aniso}}| = 0.11\%$ . The structural phase transition at  $T^*$  does not markedly affect the position or shape of the Cd-NMR spectrum. Therefore, this transition does not mark the onset of magnetic long-range order, e.g., Néel order.

Figure 3 shows a so-called  $K$ - $\chi$  plot, where values of the isotropic Knight shift  $K_{\text{iso}} = (K_{\parallel} + 2K_{\perp})/3$  are plotted against the observed susceptibility, after subtracting a Curie term that comes from a small concentration of magnetic impurities, with temperature as an implicit parameter. The linear  $K$ - $\chi$  behavior below  $T^*$ , as seen in Fig. 3, suggests that the spin component produces a shift at the Cd and that all other temperature dependences in  $K$  and  $\chi$  are negligibly small. Usually, the total shift  $K_{\text{obs}}$  in metallic compounds is composed of several contributions. In  $\text{Cd}_2\text{Re}_2\text{O}_7$ , according to band calculations,<sup>6</sup> the Fermi energy  $E_F$  locates around the valley of the Re  $5d$  band. Hence, the paramagnetic contribution is dominated by the  $5d$  spin part  $K_{\text{spin}}(T)$ , and the diamagnetic contribution  $K_{\text{dia}}$  from the core electrons is usually neglected. Further, any orbital shift for the Cd sites is expected to be small. Therefore,  $K_{\text{obs}} \approx K_{\text{spin}}(T)$ . In the same way, the observed susceptibility contains the  $5d$ -spin and  $5d$ -orbital terms  $\chi_{\text{spin}}$  and  $\chi_{\text{orb}}$ , as well as a diamagnetic term  $\chi_{\text{dia}}$  due to the core electrons, i.e.,  $\chi_{\text{obs}} = \chi_{\text{spin}}(T) + \chi_{\text{orb}} + \chi_{\text{dia}}$ , where the  $\chi_{\text{orb}}$  and  $\chi_{\text{dia}}$  are temperature independent. The diamagnetic term  $\chi_{\text{dia}}$  can be evaluated to be  $-9.0 \times 10^{-5}$  emu/Re mol from relativistic Hartree-Fock calculations.<sup>19</sup> Since  $K_{\text{spin}} \propto A_{\text{HF}} \chi_{\text{spin}}$ , the values of hyperfine (HF) coupling constant  $A_{\text{HF}}$  are estimated from the solid line in Fig. 3 to be  $+198$  kOe/ $\mu_B$  below  $T^*$ . It is difficult to resolve the small change of  $A_{\text{HF}}$  above  $T^*$ , because  $\chi_{\text{spin}}$  varies only slightly as seen in Fig. 1. One explanation for the change of the  $A_{\text{HF}}$  may be that there are Ruderman-Kittel-Kasuya-Yosida (RKKY) oscillations which couple the Cd nuclei to their neighboring Re  $5d$  spin polarization. Thus, the distance between Cd and Re sites, which varies continuously through  $T^*$ , would produce a varying coupling constant. At low temperatures, the  $\chi$ -axis intercept of the  $K$ - $\chi$  plot indicates the presence of a large Re-site Van Vleck susceptibility  $\chi_{\text{orb}}$ . This is denoted by solid arrows at the bottom of Fig. 3. We interpret the decrease of the total susceptibility below  $T^*$  as corresponding to that of the spin susceptibility.

Considering next the  $T_1$  process, we first examine the behavior at high temperatures. Figure 4 shows  $T_1^{-1}$  to be increasing linearly at 300 K, as expected for Korringa-like relaxation in a metal. Approaching the degeneracy temperature ( $\geq 300$  K), however, one might expect  $T_1$  to be dominated by exchange-modulated local-moment fluctuations on neighboring Re sites, sensed through RKKY-like transferred HF couplings. To estimate this process, we suppose that the latter consist of six equal contributions from neighboring Re  $5d$  spins whose fluctuations are uncorrelated. The exchange-narrowing theory of Moriya<sup>20</sup> would then give  $T_1^{-1} = 6T_{1S}^{-1}$ , where  $T_{1S}^{-1} = (2\pi)^{1/2} (A_S/\hbar)^2 S(S+1)/(3\omega_{\text{ex}})$ . Here,  $A_S$  is the HF coupling of a single neighbor, and we estimate  $\omega_{\text{ex}} \sim 1.4 \times 10^{14}$  sec $^{-1}$  from the CW temperature  $\Theta \sim 1500$  K ( $S=1$ ). From Fig. 3, we note that above  $T^*$ ,  $A_{\text{HF}}$  is reduced from its low-temperature value. Thus, we may estimate roughly  $A_S/\hbar \sim 2 \times 10^8$  sec $^{-1}$ . With these approximate numbers, the high-temperature limit becomes  $T_1^{-1} \sim 3 \times 10^3$  sec $^{-1}$ , about an order of magnitude larger than the 300 K value. This is a reasonable result, which under-

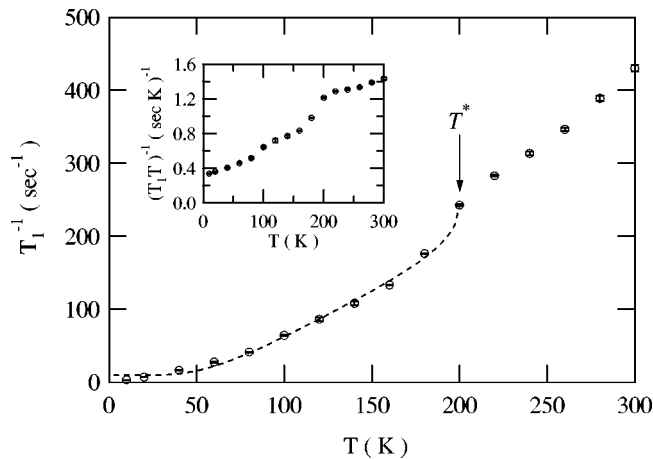


FIG. 4. Temperature dependence of  $T_1^{-1}$  for  $^{111}\text{Cd}$  nuclei in  $\text{Cd}_2\text{Re}_2\text{O}_7$ . The dotted line is drawn as a guide to eye. The inset shows the temperature dependence of  $(T_1T)^{-1}$  for  $^{111}\text{Cd}$  nuclei in  $\text{Cd}_2\text{Re}_2\text{O}_7$ .

scores the itinerant nature of the fermion dynamics at 300 K and below, in spite of the “local moment” character of the Re  $5d$  bands noted earlier.

The variation of  $T_1$  at low temperatures (Fig. 4) is the most interesting, and is not in keeping with the behavior of a simple Fermi liquid. The inset to Fig. 4 shows that  $(T_1T)^{-1}$  declines by a factor  $\sim 3$  below 200 K and has a slight bump around 125 K, the origin of which is not clear. Correspondingly, the spin susceptibility and NMR shift component (Fig. 3) also decline in such a way that the Korringa product  $(T_1TK_{\text{spin}}^2)^{-1}$  remains approximately constant below 200 K at 25–30% of its noninteracting electron value. This behavior exhibits a close parallel to that of  $^{89}\text{Y}$  NMR data for  $\text{YBa}_2\text{Cu}_3\text{O}_{7-x}$  with  $x \sim 0.3\text{--}0.4$ .<sup>21</sup> While the low- $T$  reduction of  $K_{\text{spin}}$  and  $(T_1T)^{-1}$  may or may not be a consequence of a superconducting pseudogap<sup>22</sup> (as is believed to be the case for cuprate superconductors), these effects appear to be

definite evidence that a significant portion of the Fermi surface becomes gapped below  $T^*$ .<sup>18</sup> Alternatively, the tetramerization noted earlier (Fig. 2) may also lead to a partial gapping of the Fermi surface. For example, the reduction by 2/3 or more in  $(T_1T)^{-1}$  corresponds to a loss of  $\sim 40\%$  or more of the density of states between  $T^*$  and 4.2 K, similar to estimates based on other data.<sup>18</sup> We suggest further that the reduced value of the Korringa product could originate in the same way as for  $^{89}\text{Y}$  in  $\text{YBa}_2\text{Cu}_3\text{O}_{7-x}$ ,<sup>21</sup> i.e., from the action of weakly correlated, transferred HF field fluctuations from nearest-neighbor Re sites considered above in discussing the limiting high-temperature  $T_1$  process. For example, in the case of  $T_1$  driven by  $n$  equal transferred HF couplings with uncorrelated fluctuations, the Korringa product would be diminished by a factor  $n$ . In the scenario described in the previous paragraph we have  $n \sim 6$  for  $\text{C}_2\text{Re}_2\text{O}_7$ , which easily accounts for the observed reduction of the Korringa product by a factor  $\sim 4$ . We believe that this mechanism offers a simpler and perhaps more intuitive mechanism to explain the observed Korringa product than ferromagnetic exchange couplings in a Stoner enhancement model<sup>23</sup> in view of the strongly antiferromagnetic CW temperature.

In summary, we have investigated the structural transition and the change of electronic state at  $T^*$  by using XRD, TEM, and Cd NMR, especially from the standpoint of magnetic properties. An alternating tetramerization model has been proposed in the LT phase from structural studies. The geometrical spin frustration of the pyrochlore lattice may be partially released in the LT phase due to the tetramerization. The Cd-NMR study reveals the presence of a Fermi-surface energy-gap effect in the LT phase.

This study was supported by a Grant-in-Aid on priority area, “Novel Quantum Phenomena in Transition Metal Oxides,” from MEXT, and also by a Grant-in-Aid for Scientific Research of the JSPS (Grants Nos. 12440195 and 12874038).

\*Also at Department of Chemistry, Graduate School of Science, Kyoto University, Kyoto 606-8502, Japan. Electronic address: piros@popsvr.tokai.jaeri.go.jp

<sup>1</sup>H. Sakai *et al.*, J. Phys.: Condens. Matter **13**, L785 (2001).

<sup>2</sup>M. Hanawa *et al.*, Phys. Rev. Lett. **87**, 187001 (2001).

<sup>3</sup>M.A. Subramanian *et al.*, Prog. Solid State Chem. **15**, 55 (1983).

<sup>4</sup>S. Kondo *et al.*, Phys. Rev. Lett. **78**, 3729 (1997).

<sup>5</sup>M. Hanawa *et al.*, J. Phys. Chem. Solids **63**, 1027 (2002).

<sup>6</sup>H. Harima, J. Phys. Chem. Solids **63**, 1035 (2002).

<sup>7</sup>K. Blacklock and H.W. White, J. Chem. Phys. **71**, 5287 (1979).

<sup>8</sup>H. Sakai *et al.*, in *Proceedings of the Fourteenth International Symposium on Superconductivity*, edited by T. Kobayashi and T. Morishita (Elsevier Science B. V., Kobe, 2001).

<sup>9</sup>R. Jin *et al.*, Phys. Rev. B **64**, 180503(R) (2001).

<sup>10</sup>S. Yoshii and M. Sato, J. Phys. Soc. Jpn. **68**, 3034 (1999).

<sup>11</sup>M. Ito *et al.*, J. Phys. Soc. Jpn. **69**, 888 (2000).

<sup>12</sup>H.S. Jarett *et al.*, in *Valence Instabilities and Related Narrow-Band Phenomena*, edited by R.D. Parks (Plenum, New York, 1977), p. 545.

<sup>13</sup>H. Sakai *et al.*, J. Phys. Soc. Jpn. **71**, 422 (2002).

<sup>14</sup>A.J. García-Adeva and D.L. Huber, Phys. Rev. Lett. **85**, 4598 (2000).

<sup>15</sup>M. Kontani *et al.*, Solid State Commun. **18**, 2151 (1976).

<sup>16</sup>K. Yoshimura *et al.*, J. Phys. Soc. Jpn. **57**, 409 (1988).

<sup>17</sup>N. Inoue and H. Yasuoka, Solid State Commun. **30**, 341 (1979).

<sup>18</sup>R. Jin *et al.*, cond-mat/0108402 (unpublished).

<sup>19</sup>L.B. Mendelsohn and F. Biggs, Phys. Rev. A **2**, 1130 (1970).

<sup>20</sup>T. Moriya, Prog. Theor. Phys. **16**, 33 (1956).

<sup>21</sup>H. Alloul *et al.*, Phys. Rev. Lett. **63**, 1700 (1989).

<sup>22</sup>J. Friedel, Physica C **153-155**, 1610 (1988).

<sup>23</sup>O. Vyaselev *et al.*, Phys. Rev. Lett. **89**, 017001 (2002).